Received: 7 October 2022 | Accepted: 25 November 2022

DOI: 10.1002/pamm.202200113

Closed-form buckling analysis of unsymmetrically laminated plates

Philip Schreiber[1,*] and **Christian Mittelstedt**[1]

[1] Technical University of Darmstadt, Department of Mechanical Engineering, Institute for Lightweight Construction and Design, Otto-Berndt-Straße 2, 64287 Darmstadt

The local stability of thin-walled fibre-reinforced plastic composite beams can be reduced to individual laminates using discrete plate theory. These individual plates receive a supporting effect from their surrounding structure, which is modelled with rotational restraints. In the present investigation, this buckling problem is described by a closed-form solution. The energy-based method works with the Rayleigh quotient and the principle of the stationary value of the elastic potential energy. For the analysis of unsymmetrically laminated plates, the classical laminated plate theory (CLPT) considers both the plate deflection and the in-plane displacements. The first-order shear deformation theory (FSDT) and third-order shear deformation theory (TSDT) additionally describe the cross-sectional rotations and thus take transverse shear deformations into account. In addition to the direct consideration of the bending-extension couplings, these have also been investigated using the reduced bending stiffness (RBS) method. The investigation shows the influence of bending-extension coupling on the stability of compressively loaded unsymmetrically laminated plates. Moreover, it is found that the transverse shear stiffness reduces the critical load at relatively high plate thicknesses. The closed-form analytical solution and the RBS method show good agreement with finite element analyses. The presented closed-form analytical methods provide explicit solutions for the critical compressive load of unsymmetric laminates under different boundary conditions. Due to the explicit solution, this method is significantly more computationally efficient than numerical, semi-analytical or exact methods. The present methods are characterised by a simple applicability as well as a very high computational efficiency and are very suitable for preliminary design as well as optimisation of laminated structures.

1 Introduction

Fibre composites have excellent strength and stiffness properties at low density, which makes them ideal for lightweight structures. These are mostly composed of plate-shaped layered structures called laminates. These laminates consist of very strong and stiff fibres and a comparatively flexible plastic matrix. Because of the in-plane fibre direction, the laminates have a comparatively low transverse stiffness. This can lead to high transverse shear deformations, which depend on the transverse shear stiffness as well as on the plate thickness. Consequently, the transverse shear deformation cannot be neglected in many cases. The cross-sectional deformation is described differently in the various laminated plate theories. The classical laminated plate theory (CLPT) neglects the transverse shear deformations, i.e. the cross-section remains flat and perpendicular to the mid-plane, see [1]. This is satisfied in a good approximation only for thin laminates. First order shear deformation theory (FSDT) assumes constant transverse shear deformations and gives realistic results even for thicker laminates, see [2–4]. Third order shear deformation theory (TSDT) describes cubic cross-sectional deformations, which is a more realistic model, see [5, 6]. Therefore, TSDT is also suitable for very thick laminates as well as for laminates with low transverse shear stiffnesses.

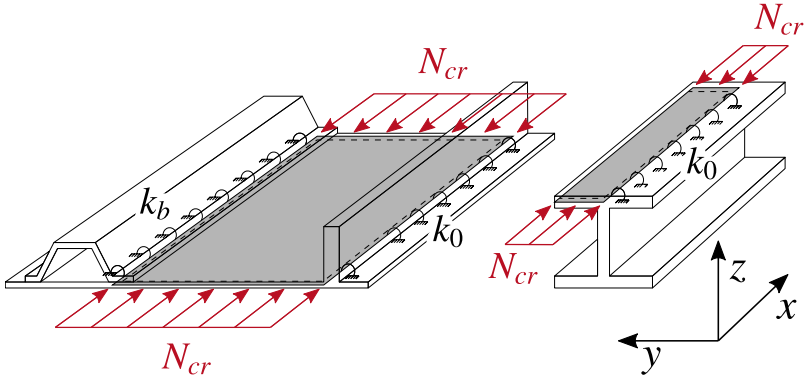

Fig. 1: Discrete plate analysis applied to the example of a stiffened plate with the SRSR plate (left) and an I-beam with the SFSR plate (right).

The lightweight design of laminates generally leads to thin-walled structures. These structures have to be investigated on their stability, which means performing linear buckling analyses. One way of doing this analytically is the so-called discrete plate analysis, in which the structure is divided into individual plates and the surrounding structure is modelled with rotational

* Corresponding author: e-mail philip.schreiber@klub.tu-darmstadt.de, phone +49 6151 16 22028, fax +49 6151 16 21980

elastic restraints. The restraint stiffness can be calculated, for example, as in [7]. These calculations can be performed extremely efficiently with closed-form analytical methods. For laminates with rotational elastic restraints and symmetrical othotropic laminate properties, such procedures can be found in [7–9] as well as [10, 11] and [12, 13] for CLPT, FSDT and TSDT, respectively. The high computational efficiency of these methods plays an important role especially for laminated structures, as they have significantly more design parameters than isotropic structures. This class of methods is excellent for design studies, preliminary design and optimisation. The present method provides an explicit solution of the critical load and extends the previously shown procedures to unsymmetric cross-ply and antisymmetric angle-ply laminates in the context of CLPT, FSDT and TSDT. The presented method is an short version of [14], detailed information about the method can be found in here.

2 Closed-form solution

The present method describes the buckling behaviour and buckling resistance of the compressively loaded laminates that are shown in Fig. 1. The first of the two boundary conditions considered is a laminated plate that is simply supported at all edges and has torsional elastic restraints at the two unloaded edges. This laminate is denoted as SRSR. The second laminate has no support on one unloaded edge instead, this is a free edge and the laminate is called SFSR. In addition, two different laminate types are considered in this study. Due to the fact that the unsymmetric cross-ply (CP) and the antisymmetric angle-ply (AP) laminates have different bending-extension couplings, it is necessary to specify distinct in-plane boundary conditions for the purely analytical description of the problem. The boundary conditions of these two cases are given below for the three considered laminate theories CLPT, FSDT and TSDT. At the boundary $x = 0, a$ applies to the simple support (S):

$$\left.\begin{array}{l}\text{CP:}\\ N^0_{xx} = v_0 = 0,\\ \text{AP:}\\ N^0_{xy} = u_0 = 0,\end{array}\right\} \left\{\begin{array}{l}\text{CLPT:}\\ w_0 = M^0_{xx} = 0\\ \text{FSDT:}\\ w_0 = M^0_{xx} = \psi_y = 0\\ \text{TSDT:}\\ w_0 = M^0_{xx} = \psi_y = P_{xx} = 0\end{array}\right. \tag{1}$$

At the edge $y = 0, b$ the following applies to the simple support with the rotational elastic restraint (R):

$$\left.\begin{array}{l}\text{CP:}\\ N^0_{yy} = u_0 = 0,\\ \text{AP:}\\ N^0_{xy} = v_0 = 0,\end{array}\right\} \left\{\begin{array}{l}\text{CLPT:}\\ w_0 = \begin{cases}\left[-M^0_{yy} - k_0 \frac{\partial w_0}{\partial y}\right]_{y=0} = 0\\ \left[M^0_{yy} - k_b \frac{\partial w_0}{\partial y}\right]_{y=b} = 0\end{cases}\\ \text{FSDT:}\\ w_0 = \psi_x = \begin{cases}\left[-M^0_{yy} + k_0\psi_y\right]_{y=0} = 0\\ \left[M^0_{yy} + k_b\psi_y\right]_{y=b} = 0\end{cases}\\ \text{TSDT:}\\ w_0 = \psi_x = P_{yy} = \begin{cases}\left[-M^0_{yy} + \frac{4}{3t^2}P_{yy} + k_0\psi_y\right]_{y=0} = 0\\ \left[M^0_{yy} - \frac{4}{3t^2}P_{yy} + k_b\psi_y\right]_{y=b} = 0\end{cases}\end{array}\right. \tag{2}$$

At the edge $y = b$ for the free edge (F) the following applies:

$$\text{CP, AP:}\quad N^0_{yy} = N^0_{xy} = 0, \quad \left\{\begin{array}{l}\text{CLPT:}\\ M^0_{yy} = \hat{Q}_y = 0\\ \text{FSDT:}\\ M^0_{yy} = M^0_{xy} = Q_y = 0\\ \text{TSDT:}\\ \begin{cases} M^0_{yy} - \frac{4}{3t^2}P_{yy} = P_{yy} = M^0_{xy} - \frac{4}{3t^2}P_{xy}\\ = \frac{4}{3t^2}\left(\frac{\partial P_{yy}}{\partial y} + 2\frac{\partial P_{xy}}{\partial x}\right) + Q_y - \frac{4}{t^2}R_y = 0\end{cases}\end{array}\right. \tag{3}$$

The displacement field of the laminated plate theories can be written as:

$$\begin{array}{lrcl}
\text{CLPT}: & u(x,y,z) & = & u_0(x,y) - z\frac{\partial w_0(x,y)}{\partial x}, \\
& v(x,y,z) & = & v_0(x,y) - z\frac{\partial w_0(x,y)}{\partial y}, \\
& w(x,y,z) & = & w_0(x,y). \\
\text{FSDT}: & u\left(x,y,z\right) & = & u_0\left(x,y\right) + z\psi_x\left(x,y\right), \\
& v\left(x,y,z\right) & = & v_0\left(x,y\right) + z\psi_y\left(x,y\right), \\
& w\left(x,y\right) & = & w_0\left(x,y\right). \\
\text{TSDT}: & u(x,y,z) & = & u_0(x,y) + z\psi_x(x,y) - \frac{4z^3}{3t^2}\left(\psi_x(x,y) + \frac{\partial w_0(x,y)}{\partial x}\right), \\
& v(x,y,z) & = & v_0(x,y) + z\psi_y(x,y) - \frac{4z^3}{3t^2}\left(\psi_y(x,y) + \frac{\partial w_0(x,y)}{\partial y}\right), \\
& w(x,y) & = & w_0(x,y).
\end{array} \tag{4}$$

The method is using a single-term Ritz method, also known as Rayleigh quotient, to describe the buckling problem of the SRSR and SFSR plates from Fig. 1. In order to achieve this, corresponding shape functions of the displacement quantities from the deflected system are considered. Each of the displacement quantities contains a single Ritz constant (U, V, W, X, Y) and the functions are separated with respect to x and y as shown in the following equation:

$$\Phi_{1,\ldots,n} = c_{1,\ldots,n}\,\Phi^{(1)}_{1,\ldots,n}\left(x\right)\Phi^{(2)}_{1,\ldots,n}\left(y\right), \begin{cases} n=3 & \text{for CLPT} \\ n=5 & \text{for FSDT} \\ & \text{and TSDT} \end{cases} \tag{5}$$

with

$$\Phi_i = \begin{bmatrix} u_0\left(x,y\right) \\ v_0\left(x,y\right) \\ w_0\left(x,y\right) \\ \psi_x\left(x,y\right) \\ \psi_y\left(x,y\right) \end{bmatrix}, \quad c_i = \begin{bmatrix} U \\ V \\ W \\ X \\ Y \end{bmatrix}, \quad \Phi^{(1)}_i = \begin{bmatrix} u_1\left(x\right) \\ v_1\left(x\right) \\ w_1\left(x\right) \\ \psi_{x_1}\left(x\right) \\ \psi_{y_1}\left(x\right) \end{bmatrix}, \quad \Phi^{(2)}_i = \begin{bmatrix} u_2\left(y\right) \\ v_2\left(y\right) \\ w_2\left(y\right) \\ \psi_{x_2}\left(y\right) \\ \psi_{y_2}\left(y\right) \end{bmatrix}.$$

The approaches are selected in such a way that they represent the buckling shape according to the different boundary conditions. In the x-direction sine as well as cosine functions and in the y-direction polynomials of third as well as fourth order have been chosen. These functions allow different values of restraint stiffness at the unloaded edges. Due to the different in-plane boundary conditions, the approaches of unsymmetric cross-ply and antisymmetric angle-ply laminates are different in the displacements u_0 and v_0. For the cross-ply laminate these are:

$$\begin{aligned}
u_1 &= \cos\left(\tfrac{m\,\pi\,x}{a}\right), \quad u_2 = \left(\tfrac{y}{b}\right) + W_2\left(\tfrac{y}{b}\right)^2 + W_3\left(\tfrac{y}{b}\right)^3 + W_4\left(\tfrac{y}{b}\right)^4, \\
v_1 &= \sin\left(\tfrac{m\,\pi\,x}{a}\right), \quad v_2 = 1 + 2\,W_2\left(\tfrac{y}{b}\right) + 3\,W_3\left(\tfrac{y}{b}\right)^2 + 4\,W_4\left(\tfrac{y}{b}\right)^3.
\end{aligned} \tag{6}$$

The approaches of the antisymmetric angle-ply laminate show the following structure:

$$\begin{aligned}
u_1 &= \sin\left(\tfrac{m\,\pi\,x}{a}\right), \quad u_2 = 1 + 2\,W_2\left(\tfrac{y}{b}\right) + 3\,W_3\left(\tfrac{y}{b}\right)^2 + 4\,W_4\left(\tfrac{y}{b}\right)^3, \\
v_1 &= \cos\left(\tfrac{m\,\pi\,x}{a}\right), \quad v_2 = \left(\tfrac{y}{b}\right) + W_2\left(\tfrac{y}{b}\right)^2 + W_3\left(\tfrac{y}{b}\right)^3 + W_4\left(\tfrac{y}{b}\right)^4.
\end{aligned} \tag{7}$$

For the remaining quantities, the approaches are identical and read as follows:

$$\begin{aligned}
w_1 &= \sin\left(\tfrac{m\,\pi\,x}{a}\right), \quad w_2 = \left(\tfrac{y}{b}\right) + W_2\left(\tfrac{y}{b}\right)^2 + W_3\left(\tfrac{y}{b}\right)^3 + W_4\left(\tfrac{y}{b}\right)^4, \\
\psi_{x_1} &= \cos\left(\tfrac{m\,\pi\,x}{a}\right), \quad \psi_{x_2} = \left(\tfrac{y}{b}\right) + W_2\left(\tfrac{y}{b}\right)^2 + W_3\left(\tfrac{y}{b}\right)^3 + W_4\left(\tfrac{y}{b}\right)^4, \\
\psi_{y_1} &= \sin\left(\tfrac{m\,\pi\,x}{a}\right), \quad \psi_{y_2} = 1 + 2\,W_2\left(\tfrac{y}{b}\right) + 3\,W_3\left(\tfrac{y}{b}\right)^2 + 4\,W_4\left(\tfrac{y}{b}\right)^3.
\end{aligned} \tag{8}$$

The approaches obtained in this way are substituted into the total potential energy of the laminate, which is composed of the inner potential, the external potential and the potential of the rotational elastic restraint:

$$\Pi = \Pi_\mathrm{i} + \Pi_\mathrm{a} + \Pi_\mathrm{s}. \tag{9}$$

The individual components can be described as:

$$\Pi_{\mathrm{i}} = \frac{1}{2}\int_0^b \int_0^a \underline{\varepsilon}^{\mathrm{T}}\underline{\overline{N}}\,\mathrm{d}x\,\mathrm{d}y, \tag{10}$$

$$\Pi_{\mathrm{a}} = -\frac{N_{\mathrm{cr}}}{2}\int_0^b \int_0^a \left\{\xi_x\left(\frac{\partial w_0}{\partial x}\right)^2 + \xi_y\left(\frac{\partial w_0}{\partial y}\right)^2\right\}\mathrm{d}x\,\mathrm{d}y, \tag{11}$$

$$\Pi_{\mathrm{s}} = \frac{1}{2}\int_0^a \int_{-t/2}^{t/2} \left\{\frac{k_0}{t}\left[\overline{\varphi}^2\right]_{y=0} + \frac{k_b}{t}\left[\overline{\varphi}^2\right]_{y=b}\right\}\mathrm{d}z\,\mathrm{d}x \tag{12}$$

with

$$\overline{\varphi} = \frac{\partial v(x,y,z)}{\partial z}. \tag{13}$$

The plate dimensions length, width and thickness are given as a, b and t respectively. Substituting the approaches (5) into the corresponding total potential of CLPT, FSDT or TSDT allows the extraction of Ritz's constants and leads to the following form for all laminated plate theories:

$$\Pi = \frac{1}{2}\,\underline{c}^{\mathrm{T}}\underline{\underline{\Lambda}}\,\underline{c} = \frac{1}{2}\,\Lambda_{ij}c_jc_i, \begin{cases} i,j = 1,2,3 & \text{for CLPT} \\ i,j = 1,..,5 & \text{for FSDT} \\ & \text{and TSDT} \end{cases} \tag{14}$$

with

$$\Lambda_{ij} = \begin{bmatrix} \lambda_{11} & \lambda_{12} & \lambda_{13} & \lambda_{14} & \lambda_{15} \\ \lambda_{12} & \lambda_{22} & \lambda_{23} & \lambda_{24} & \lambda_{25} \\ \lambda_{13} & \lambda_{23} & N_{\mathrm{cr}}\overline{\lambda}_{33} + \lambda_{33} & \lambda_{34} & \lambda_{35} \\ \lambda_{14} & \lambda_{24} & \lambda_{34} & \lambda_{44} & \lambda_{45} \\ \lambda_{15} & \lambda_{25} & \lambda_{35} & \lambda_{45} & \lambda_{55} \end{bmatrix}, \begin{cases} i,j = 1,2,3 \\ \text{for CLPT} \\ i,j = 1,..,5 \\ \text{for FSDT} \\ \text{and TSDT} \end{cases} \tag{15}$$

In the matrix $\underline{\underline{\Lambda}}$ the integral expressions and the stiffness parameters are collected. A detailed description of these expressions can be found in [14].

The system is in a state of equilibrium according to the principle of the stationary value of the elastic potential energy. This can be described for the deflected plate with the Ritz equations, which read as follows:

$$\frac{\partial \Pi}{\partial c_i} = \Lambda_{ij}c_j = 0, \begin{cases} i,j = 1,2,3 & \text{for CLPT} \\ i,j = 1,..,5 & \text{for FSDT} \\ & \text{and TSDT} \end{cases} \tag{16}$$

This results in a linear system of equations which represents an eigenvalue problem with respect to the critical load. For its solution, the vanishing of the coefficient matrix determinant is required:

$$\det(\Lambda_{ij}) = 0. \tag{17}$$

These conditions result in an equation that can be solved for the critical load N_{cr}, which for the CLPT results in:

$$N_{\mathrm{cr}} = -\frac{\lambda_{11}\lambda_{22}\lambda_{33} - \lambda_{11}{\lambda_{23}}^2 - {\lambda_{12}}^2\lambda_{33} + 2\,\lambda_{12}\lambda_{13}\lambda_{23} - {\lambda_{13}}^2\lambda_{22}}{\overline{\lambda}_{33}\left(\lambda_{11}\lambda_{22} - {\lambda_{12}}^2\right)}. \tag{18}$$

For FSDT and TSDT, the solution can be defined using the Levi-Civita symbol ε_{ijklm} as follows:

$$N_{\mathrm{cr}} = -\frac{\sum_{i=1}^{5}\sum_{j=1}^{5}\sum_{k=1}^{5}\sum_{l=1}^{5}\sum_{m=1}^{5}\varepsilon_{ijklm}\lambda_{1i}\lambda_{2j}\lambda_{3k}\lambda_{4l}\lambda_{5m}}{\sum_{i=1}^{5}\sum_{j=1}^{5}\sum_{l=1}^{5}\sum_{m=1}^{5}\varepsilon_{ij3lm}\lambda_{1i}\lambda_{2j}\overline{\lambda}_{33}\lambda_{4l}\lambda_{5m}}. \tag{19}$$

Due to the explicit representations of the solutions, this method is significantly more computationally efficient than numerical, semi-analytical or exact methods and straightforward to implement.

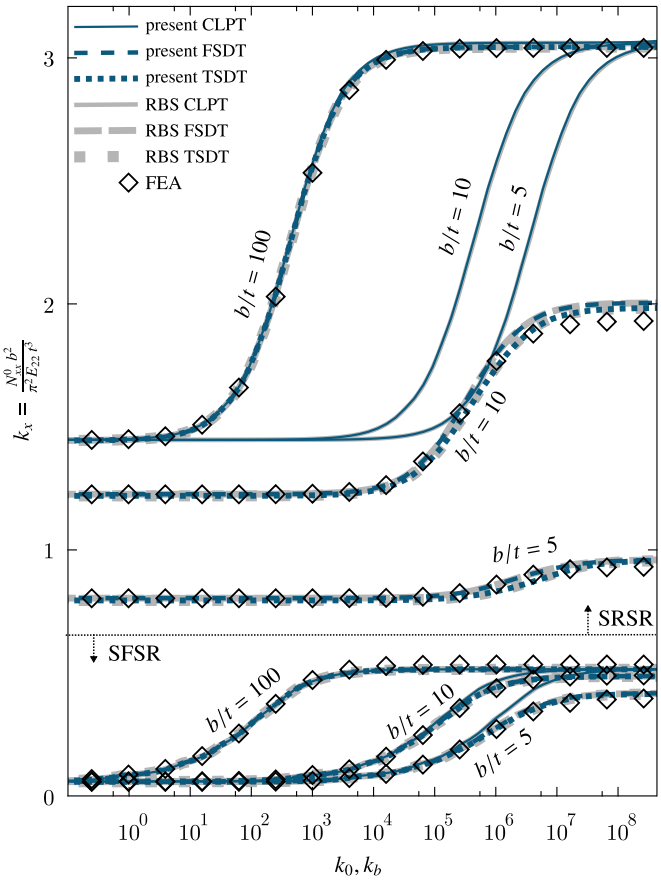

Fig. 2: Cross-ply $[(0^\circ/90^\circ)_2]$: The non-dimensional buckling load k_x is given as a function of the rotational restraints k_0, k_b for different relative widths b/t $(5, 10, 100)$ and the boundary conditions SRSR and SFSR with the aspect ratio of $a/b = 10$. Graphic is taken from [14].

3 Results

The present analytical method (CF) is verified by finite element analysis (FEA) of single plates with rotational restraints. Results from the RBS method are also included in the analysis. Here, the bending stiffnesses have been reduced from the stiffness matrix of the constitutive law by using RBS and the laminates have subsequently been considered as symmetrical. These are then calculated using the closed-form analytical methods as well. The main difference is that once the bending-extension coupling is considered directly and in the RBS using reduced stiffnesses. In Fig. 2 the restraint stiffness (k_0, k_b) of a cross-ply laminate is investigated for different relative widths (b/t). In the upper part of the graph are curves of the SRSR plate and in the lower part those of the SFSR plate. It can be observed that the analytical CLPT solutions show a good agreement for large b/t ratios, but a very large deviation for small ones. For the higher-order laminated plate theories FSDT and TSDT, good agreements between CF and RBS with FEA are observed.

The antisymmetric angle-ply laminates in the context of TSDT show very good agreement between CF and FEA in Fig. 3 for the SRSR plate on the one hand. The fibre angles are mapped very well. The RBS, on the other hand, shows larger differences for small ply repetitions n. Larger deviations are observed for the SFSR plate.

4 Conclusion

The presented methods calculate the buckling loads of laminated plates that exhibit symmetric as well as unsymmetric orthotropic behaviour, namely unsymmetric cross-ply and antisymmetric angle-ply laminates. The CLPT neglects the influence of the transverse shear deformations and consequently overestimates the critical load for small relative widths. The present CF method shows very good agreement for cross-ply laminates in direct application as well as with the RBS method. With regard to angle-ply laminates, on the one hand it can be noted that the laminate with the free edge (SFSR plate) shows larger deviations. If necessary, other methods such as a Lévy-type solution or FEA should be used. On the other hand, the RBS method shows significant deviations for small layer repetitions. Besides the cases mentioned, good agreements can be observed for the angle-ply laminates as well. Due to the explicit solution, the method shows a very high computational efficiency as well as a good applicability and is very well suited for the preliminary design and optimisation of laminated structures.

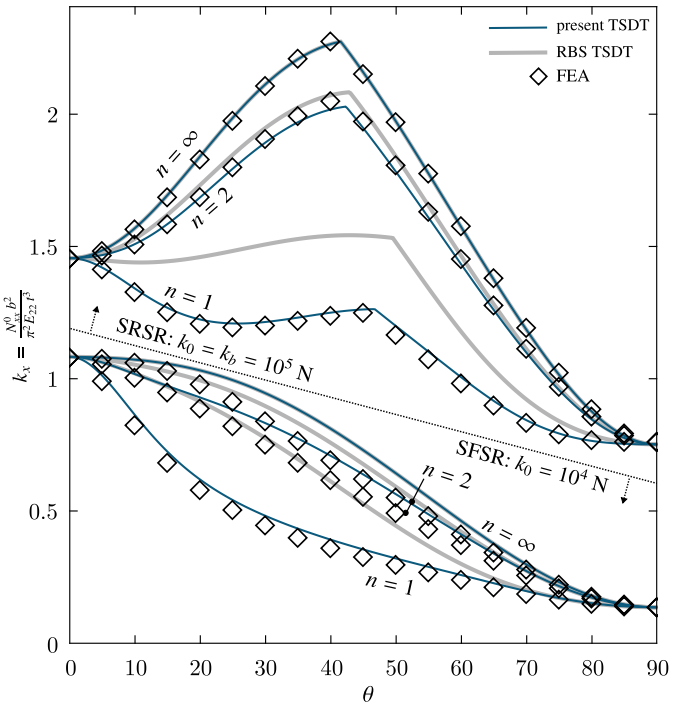

Fig. 3: Angle-ply $[(\theta^\circ/-\theta^\circ)_n]$: The non-dimensional buckling load k_x is given with respect to the ply angle θ for the relative width of $b/t = 10$ and the aspect ratio of $a/b = 1$. The ply repetitions $n = 1, 2, \infty$ for the boundary conditions SRSR and SFSR with the rotational elastic restraints $k_0 = k_b = 10^5$ N and $k_0 = 10^4$ N, respectively, are considered. Graphic is taken from [14].

Acknowledgements This work was supported by the German Research Foundation (Deutsche Forschungsgemeinschaft, DFG) [grant number 421986570]. Open access funding enabled and organized by Projekt DEAL.

References

[1] E. Reissner and Y. Stavsky, Journal of Applied Mechanics **28**(3), 402–408 (1961).
[2] P. Yang, C. H. Norris, and Y. Stavsky, International Journal of Solids and Structures **2**(4), 665–684 (1966).
[3] J. M. Whitney and N. J. Pagano, Journal of Applied Mechanics **37**(4), 1031–1036 (1970).
[4] T. S. Chow, Journal of Composite Materials **5**(3), 306–319 (1971).
[5] J. N. Reddy, Journal of Applied Mechanics **51**(4), 745–752 (1984).
[6] J. N. Reddy, International Journal of Solids and Structures **20**(9-10), 881–896 (1984).
[7] P. Qiao and L. Shan, Composite Structures **70**(4), 468–483 (2005).
[8] L. P. Kollár, Journal of Structural Engineering **128**(9), 1202–1211 (2002).
[9] C. Mittelstedt, Composite Structures **81**(4), 550–558 (2007).
[10] T. Kuehn, H. Pasternak, and C. Mittelstedt, Composite Structures **113**, 236–248 (2014).
[11] M. Beerhorst and S. Thirusala Suresh Babu, Composite Structures **240**, 112037 (2020).
[12] J. Herrmann, T. Kühn, T. Müllenstedt, S. Mittelstedt, and C. Mittelstedt, International Journal of Structural Stability and Dynamics **18**(11), 1850139–1–30 (2018).
[13] P. Schreiber, C. Mittelstedt, and M. Beerhorst, Thin-Walled Structures **157**, 107071–1–14 (2020).
[14] P. Schreiber and C. Mittelstedt, International Journal of Mechanical Sciences **218**, 106995 (2022).

